Desalination 281 (2011) 199–208

Contents lists available at ScienceDirect

Desalination

journal homepage: www.elsevier.com/locate/desal

Validation of an analytical model for spiral wound reverse osmosis membrane module using experimental data on the removal of dimethylphenol

G. Srinivasan [a,1], S. Sundaramoorthy [a,*], D.V.R. Murthy [b,2]

[a] Department of Chemical Engineering, Pondicherry Engineering College, Pondicherry, 605014, India
[b] Department of Chemical Engineering, National Institute of Technology, Karnataka, Surathkal, 575025, India

ARTICLE INFO

Article history:
Received 1 May 2011
Received in revised form 25 July 2011
Accepted 26 July 2011
Available online 16 August 2011

Keywords:
Reverse Osmosis
Spiral-wound module
Analytical model
Parameter estimation
Dimethylphenol

ABSTRACT

A new analytical model for spiral wound RO module has been recently proposed by Sundaramoorthy et al. [1] and the same has been validated [2] with experimental data obtained on a laboratory scale RO unit used for the removal of chlorophenol. In this paper, the need to check the validity of this model with solutes other than chlorophenol is addressed by conducting suitable experiments with dimethylphenol as solute and validating this experimental data with the model. The four model parameters namely solvent transport coefficient A_w, solute transport coefficient Bs, feed channel friction parameter b and the mass transfer coefficient k were estimated. The results show that the mass transfer coefficient is influenced not only by fluid velocity but also by the solvent flux and solute concentration. A new correlation for mass transfer coefficient k, proposed by Sundaramoorthy et al. [2] for experimental data taken with chlorophenol as solute is also shown to be consistent with the experimental readings recorded in this study taking dimethylphenol as solute. Comparison of model predictions with the experimental observations demonstrated the capability of the model in predicting permeate concentration within 12% error, retentate flow within 5% error and rejection coefficient within 2% error.

1. Introduction

In the past 20 years, Reverse Osmosis (RO) has emerged as a successful technology for the removal of organic compounds and its application in water and waste water treatment has become wide spread [3,4]. Application of RO in the removal of phenolic compounds is of specific interest in the treatment of industrial effluents as phenol and phenolic compounds are used as raw materials for synthesis of a number of chemical products including antiseptics, disinfectants, pesticides, herbicides, pharmaceuticals, dyes, pigments and paints. A number of studies on the removal of phenol, chlorophenol, and alkyl phenols using RO have been reported in the literature [5–9]. The research work presented in this paper is on the removal of dimethylphenol using Thin Film Composite (TFC) polyamide RO membrane. Dimethylphenol is an important organic aromatic compound that appears in waste water from various industrial activities such as petroleum processing, plastic manufacturing and production of resins.

With increasing applications of RO in the removal of organic compounds, studies on the performance of RO modules in the removal of organic compounds have gained importance. Industrial RO units are commonly available in three basic modular designs, namely plate and frame module, hollow-fiber module and spiral wound module [10,11]. Of these three modular designs, the spiral-wound module is widely used due to high packing density, moderate fouling resistance and lower capital and operating costs [12]. This paper deals with the performance analysis of a laboratory scale spiral-wound RO module used for the removal of dimethylphenol.

Appropriate mathematical model is essential to predict the performance of a spiral-wound RO module under various operating conditions. Models for describing the performance of membrane modules are broadly classified as '*Approximate Analytical Models*' that typically assume average conditions on either side of the membrane and '*Rigorous Numerical Models*' that account for spatial variations in fluid properties throughout the module. Although numerical models are appropriate for describing complex situations, the analytical models are more useful for gaining better physical insight and understanding of the system.

Simple analytical design equations for the calculation of channel length and average permeate concentration in spiral wound RO modules were reported by Sirkar et al. [13]. In this work, pressure drop in feed and permeate channels were neglected and a linear approximation for concentration polarization term $e^{Jv/k}$ was assumed. Neglecting pressure drops in both feed and permeate channels and assuming the value of mass transfer coefficient k to be same throughout the channel length, Gupta et al. [14] developed analytical

* Corresponding author. Tel.: +91 9444290056; fax: +91 413 2655101.
E-mail addresses: seenu_pec@yahoo.com (G. Srinivasan), ssm_pec@yahoo.com (S. Sundaramoorthy), dvrmvzm@gmail.com (D.V.R. Murthy).
[1] Tel.: +91 9444290056; fax: +91 413 2655101.
[2] Tel.: +91 824 2474039; fax: +91 824 2474033.

0011-9164/$ – see front matter © 2011 Elsevier B.V. All rights reserved.
doi:10.1016/j.desal.2011.07.053

design equations for spiral wound RO modules. Ignoring the spatial variations of pressure and solute concentrations in both the channels, Evangelista and Jonsson [15] and Evangelista [16] derived explicit analytical equations for water flux and validated these equations for dilute solutions. All these analytical models mentioned above are based on assumptions of average and uniform fluid conditions in feed and permeate channels. Avlontis et al. [17,18] proposed an analytical solution for the spiral wound RO modules, which was the first analytical model reported in the literature that accounted for spatial variations in pressure, velocity and concentration in both the feed and permeate channels. However, this analytical model assumed a constant value for mass transfer coefficient all along the length of the module and also used a linear approximation for the concentration polarization term $e^{Jv/k}$.

Recently, Sundaramoorthy et al. [1] have proposed a new analytical model for spiral wound RO modules and reported explicit equations for spatial variations of pressure, fluid velocity and solute concentration on the feed channel side. In this model, the pressure on the permeate channel side is assumed to be uniform as the flow rate in the permeate channel is much smaller than the flow rate in the feed channel. Further this model, unlike the other analytical model reported by Avlontis et al. [17] assumes the mass transfer coefficient k to vary along the feed channel length with varying fluid properties and also treats the concentration polarization term $e^{Jv/k}$ as it is without approximating it to a linear equation. Sundaramoorthy et al. [2] have also reported studies on validation of this analytical model using experimental data on the removal of chlorophenol in a laboratory scale spiral wound RO module.

In this paper, the experimental studies on the removal of dimethylphenol in a laboratory scale spiral wound RO module are reported. The main objective of this work is to validate the analytical model for spiral wound RO module reported by Sundaramoorthy et al. [1] with the experimental data on the removal of dimethylphenol.

2. Mathematical model for the spiral wound RO module

The mathematical model reported by Sundaramoorthy et al. [1] is used in this study for characterizing the performance of the spiral wound RO module. In this work, a complete model for the spiral wound RO module was developed by combining the '*membrane transport equations*' that describe the solute and solvent flux through the membranes with the '*conservation and flow equations*' that describe the flow of fluid through the feed and the permeate channels of the module.

The solution–diffusion model [19] is assumed to explain the mechanism of solute and solvent transport through the membrane and according to this model the solvent flux J_v and solute flux J_s through the membrane are given by the following equations.

$$J_V = A_W(\Delta P - \Delta\Pi) \tag{1}$$

$$J_S = B_S(C_b - C_p) \tag{2}$$

where, A_W is the solvent transport coefficient, B_S is the solute transport coefficient, ΔP is the transmembrane pressure, which is the difference in pressures across the membrane defined as

$$\Delta P = (P_b - P_P) \tag{3}$$

where P_b and P_p are the pressures on the retentate side and permeate side of the membrane respectively $\Delta\Pi$ is the osmotic pressure difference across the membrane, C_b and C_p are respectively the solute concentrations on the retentate and permeate sides of the membrane. The osmotic pressure difference, $\Delta\Pi$ across the membrane is given by the Vant hoff's relation

$$\Delta\Pi = \gamma T(C_b - C_p) \tag{4}$$

where γ is the gas law constant and T is the temperature. The effect of concentration polarization [19] on the transport of solute and solvent through the membrane is characterized by mass transfer coefficient k. This term k relates the concentration of solute at the membrane wall C_W to the bulk solute concentration C_b on the retentate side and the solute concentration C_p on the permeate side through the following equation

$$\frac{C_W - C_p}{C_b - C_p} = e^{\left(\frac{J_v}{k}\right)}. \tag{5}$$

The variation of fluid properties (flow, pressure and solute concentration) from one end of the module to the other end is described by writing the conservation and flow equations across the feed and permeate channels of the whole module. The fluid flow rate, fluid pressure and solute concentration are assumed to vary from inlet to outlet on the feed channel side, whereas on the permeate channel side the pressure drop is neglected due to low permeate flow rate. With these assumptions, it was shown [1] that the solute and solvent conservation equations demand the permeate concentration C_p value to be uniform throughout the permeate channel. With permeate concentration C_p and permeate pressure P_p taking constant values in the permeate channel and the values of solute concentration C_b, fluid pressure P_b and fluid flow F varying along the feed channel length, the spiral wound RO module can be schematically represented by a simplified diagram shown in Fig. 1.

With the solute concentration C_p taking a constant value in the permeate channel, the solvent flux J_v (x) at a distance x from the feed channel inlet was shown to vary with local transmembrane pressure $\Delta P(x)$ according to the equation given below

$$J_v(x) = \frac{A_W.\Delta P(x)}{1 + \left(\frac{A_W\gamma}{B_S}\right)TC_p} \tag{6}$$

As the fluid flows through the feed channel, its pressure drops from P_i at inlet to P_o at outlet. This pressure drop in the feed channel is due to wall friction as well as due to the drag caused by flow past internals. Assuming the Darcy's law to be applicable, the pressure gradient $\frac{dP_b(x)}{dx}$ in the feed channel at a distance x from the inlet is proportional to the volumetric flow rate F(x)

$$\frac{dP_b(x)}{dx} = -bF(x) \tag{7}$$

where the proportionality constant b is the feed channel friction parameter. Further, the solvent balance in the feed channel section yields an expression for the solvent flux $J_v(x)$ as a function of gradient of flow rate $\frac{dF(x)}{dx}$,

$$J_v(x) = -\frac{1}{W}\frac{dF(x)}{dx} \tag{8}$$

where W is the width of the flat membrane rolled and packed into the module.

Solving the model equations listed above with appropriate boundary conditions, analytical expressions were derived for the prediction of retentate flow rate (F_o), retentate pressure (P_o), retentate concentration (C_o), permeate concentration (C_p) and solvent flux (J_v). A summary of essential analytical equations required for validation of the model [1] is presented in this section.

The equations for flow rate F(x), solvent flux $J_v(x)$, pressure $P_b(x)$ and solute concentration $C_b(x)$ in the feed channel at a distance x from the feed inlet are given below

$$F(x) = \frac{F_o \sinh\frac{\varnothing x}{L} + F_i \sinh\varnothing\left(1 - \frac{x}{L}\right)}{\sinh\varnothing} \tag{9}$$

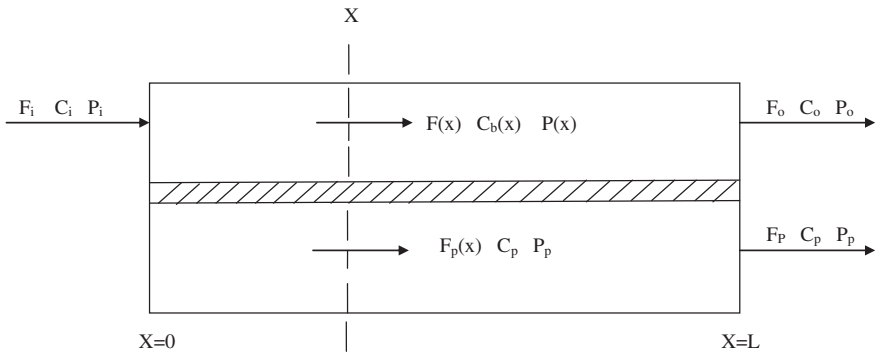

Fig. 1. Schematic representation of spiral wound reverse osmosis membrane module depicting spatial variations.

$$J_V(x) = \frac{\varnothing}{A_m \sinh\varnothing}\left[F_i \cosh\varnothing\left(1-\frac{x}{L}\right) - F_o \cosh\frac{\varnothing x}{L}\right] \tag{10}$$

$$P_b(x) = P_i - \frac{bL}{\varnothing\sinh\varnothing}\left[F_o\left(\frac{\cosh\varnothing x}{L}-1\right) - F_i\left(\cosh\varnothing\left(1-\frac{x}{L}\right)-\cosh\varnothing\right)\right] \tag{11}$$

$$C_b(x) = C_p + \frac{F_i(C_i - C_p)}{F(x)} \tag{12}$$

where, $\varnothing$ is the dimensionless parameter defined as

$$\varnothing = L\sqrt{\frac{WbA_W}{\left(1 + A_w\left(\frac{\gamma}{B_s}\right)TC_p\right)}} \tag{13}$$

where L is the length of the module. The solute flux $J_v(x)$ evaluated at $x=0$ and $x=L$ are

$$J_v(0) = \frac{A_W.\Delta P_i}{1 + \left(\frac{A_W\gamma}{B_s}\right)TC_p} \tag{14}$$

$$J_v(L) = \frac{A_W.\Delta P_o}{1 + \left(\frac{A_W\gamma}{B_s}\right)TC_p} \tag{15}$$

where ΔP_i and ΔP_o are the transmembrane pressures at $x=0$ and $x=L$ respectively

$$\Delta P_i = P_i - P_p \tag{16}$$

$$\Delta P_o = P_o - P_p \tag{17}$$

The equations for retentate flow F_o, retentate pressure P_o and retentate concentration C_o are

$$F_o = F_i\cosh\varnothing - \frac{\varnothing\sinh\varnothing}{bL}\Delta P_i \tag{18}$$

$$P_o = P_i - \frac{bL}{\varnothing\sinh\varnothing}[(F_i + F_o)(\cosh\varnothing - 1)] \tag{19}$$

$$C_o = C_p + \frac{F_i(C_i - C_p)}{F_o} \tag{20}$$

The equations for permeate concentration C_p evaluated at $x=0$ and $x=L$ are

$$C_p = \frac{C_i}{\left[1 + \frac{J_V(0)/B_s}{e^{J_V(0)/ki}}\right]} \tag{21}$$

$$C_p = \frac{C_o}{\left[1 + \frac{J_V(L)/B_s}{e^{J_V(L)/ko}}\right]} \tag{22}$$

where k_i and k_o are the mass transfer coefficients at feed channel inlet and outlet respectively.

3. Experimental studies

The experimental study on the removal of dimethylphenol in a laboratory scale spiral wound RO module is reported in this section.

3.1. Experimental setup

A commercial thin film composite polyamide RO membrane packed in a spiral wound module (Ion Exchange, India) was used for the experimental studies. Detailed specifications of the membrane module are given in Table 1. The schematic diagram of the experimental setup used in this work is shown in Fig. 2. The feed solution kept in a stainless steel feed tank (FT) was pumped through the spiral wound RO module (M) by a high pressure pump (P) capable

Table 1
Specifications of the spiral wound membrane module.

Make	Ion exchange, India
Membrane material	TFC polyamide
Module configuration	Spiral wound
Number of turns (n)	30
Feed spacer thickness (t_f), mm	0.8
Permeate channel thickness, (t_p), mm	0.5
Membrane area(A_m), m^2	7.85
Feed channel area (A_f), m^2	6.72×10^{-3}
Permeate channel area (A_p), m^2	4.67×10^{-4}
Module length (L), m	0.934
Module diameter (D), in.	3.25
Membrane width (W), m	8.40
% Salt rejection	>97%

TFC — thin film composite.

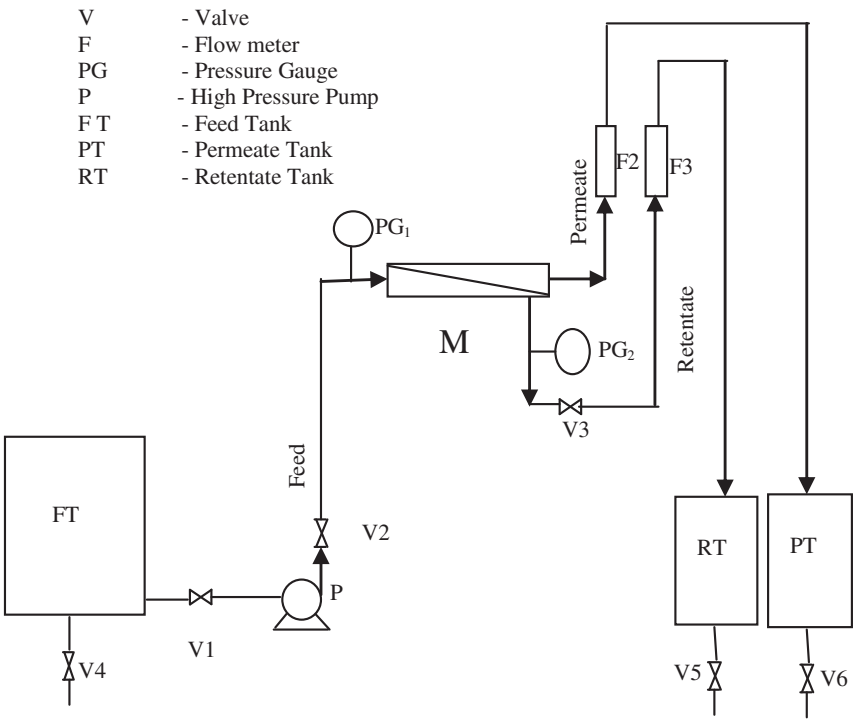

Fig. 2. Schematic diagram of the experimental set up.

of developing pressure up to 20 atm. The permeate and retentate solutions flowing out of the membrane module were collected in separate permeate (PT) and retentate (RT) collection tanks. A manual needle valve (V3) provided at the retentate outlet line was adjusted to set the fluid feed pressure. V1 and V2 are isolation valves for the high pressure pump. V4, V5 and V6 are drain valves for feed, retentate and permeate tanks respectively. Bourdon pressure gages (PG_1 and PG_2) were installed in the feed and retentate lines to measure the inlet and outlet pressures across the membrane module. Neglecting the pressure drop on the permeate side of the membrane, the pressure on the permeate side was taken as 1 atm. Permeate and retentate flow rates were measured by means of rotameters F2 and F3 and sum of these two flow rates was taken as the feed flow rate. The high pressure pump was provided with a variable frequency drive to adjust the speed of the motor and vary the feed flow rate between 7.5 LPM and 16 LPM. A HPLC (Perkin Elmer, USA) unit equipped with a UV detector and C-18 column was used for the analysis and measurement of solute (Dimethylphenol) concentrations in retentate and permeate solutions.

3.2. Experimental methods

Aqueous feed solution of dimethylphenol of specific concentration was prepared by dissolving required quantity of dimethylphenol in water. Taking around 350 l of feed solution in the feed tank (FT), the RO unit was operated at a fixed inlet pressure and a fixed feed flow rate. For each run, before collecting the samples for analysis, the unit was operated for about 40 min to ensure the attainment of steady state. Steady state readings of inlet pressure, outlet pressure, permeate flow rate and retentate flow rate were recorded. Permeate and retentate concentrations were measured by collecting the samples of permeate and retentate solutions and analyzing them using HPLC. The feed temperature was recorded by reading the thermometer kept in the feed tank.

For each experimental run, the steady state readings of permeate flow rate (F_p), retentate flow rate (F_o), retentate pressure (P_o), retentate concentration (C_o),permeate concentration (C_p) and feed temperature (T) were recorded for a set of fixed values of feed concentration (C_i), feed flow rate (F_i) and feed pressure (P_i). Experiments were conducted at three different feed flow rates (13, 14 and 15.5 LPM), five feed concentrations (100, 200, 300, 500 and 800 ppm) and five feed pressures (5.83, 7.77, 9.71, 11.64 and 13.58 atm). A total of 71 readings were collected in these experimental runs and reported in Tables 2, 3 and 4. The values of rejection coefficient R calculated using the experimental readings of C_p and C_o are also given in these tables.

$$R = 1 - \frac{C_P}{C_O} \tag{23}$$

4. Estimation of model parameters

The model for spiral wound RO module reported by Sundaramoorthy et al. [1] has four parameters. They are solvent transport coefficient A_W, solute transport coefficient B_S, mass transfer coefficient k and the feed channel fluid friction parameter b. The parameters A_W and B_S that characterize the transport of solvent and solute through the membranes are intrinsic properties of the membrane material and solvent and solute molecules. The parameter b that accounts for pressure loss due to friction in the feed channel depends on module dimensions and geometry. The fourth parameter namely the mass transfer coefficient k is strongly influenced by fluid properties as well as the operating conditions such as flow rate. Methods for estimation of these parameters from the experimental data are reported by Sundaramoorthy et al. [1]. In this work, least square methods for estimation of A_W, B_S and b are developed by writing the analytical model equations in the form of graphical linear fit.

The mass transfer coefficient k is usually estimated using standard mass transfer correlations [20,21] applicable for flow through tubes or rectangular channels. Although many investigators [22–24] have justified the application of standard mass transfer correlations for estimation of k in membrane transport, there are a few [25,26] who

Table 2
Experimental and theoretical data on removal of dimethylphenol in the spiral wound RO module at a feed flow rate of $F_i = 2.166 \times 10^{-4}$ m^3/s.

Sr. no.	P_i (atm)	P_o (atm)	T (°C)	$C_i \times 10^{+03}$ (kmol/m^3)	$F_o \times 10^{+04}$, (m^3/s)		% Error	$C_p \times 10^{+04}$, (kmol/m^3)		% Error	R		% Error
					(Expt)	(Theo)		(Expt)	(Theo)		(Expt)	(Theo)	
1	5.83	4.46	32.5	0.819	1.800	1.900	−5.319	0.931	0.962	−3.276	0.902	0.896	0.707
2	7.77	6.31	32.5	0.819	1.670	1.760	−5.125	0.864	0.868	−0.519	0.915	0.912	0.328
3	9.71	8.14	32.5	0.819	1.590	1.620	−1.641	0.790	0.831	−5.237	0.927	0.922	0.539
4	11.64	9.98	32.5	0.819	1.500	1.480	1.450	0.740	0.819	−10.714	0.936	0.929	0.653
5	13.58	11.8	32.5	0.819	1.370	1.340	2.123	0.729	0.822	−12.751	0.942	0.935	0.672
6	5.83	4.41	31	1.637	1.851	1.920	−3.466	1.526	1.541	−0.991	0.919	0.916	0.362
7	7.77	6.27	31	1.637	1.736	1.780	−2.555	1.335	1.344	−0.686	0.934	0.932	0.215
8	9.71	8.09	31	1.637	1.630	1.650	−0.984	1.209	1.256	−3.918	0.943	0.941	0.296
9	11.64	9.93	31	1.637	1.523	1.510	0.634	1.167	1.216	−4.165	0.949	0.947	0.192
10	13.58	11.76	31	1.637	1.416	1.380	2.454	1.140	1.201	−5.363	0.953	0.952	0.145
11	5.83	4.37	31	2.455	1.868	1.930	−3.356	2.575	2.270	11.840	0.908	0.924	−1.756
12	7.77	6.22	31	2.455	1.761	1.800	−2.217	2.204	1.964	10.880	0.926	0.940	−1.493
13	9.71	8.05	31	2.455	1.666	1.670	−0.221	1.778	1.624	8.652	0.943	0.948	−0.517
14	11.64	9.89	31	2.455	1.566	1.540	1.608	1.710	1.553	9.163	0.949	0.954	−0.582
15	13.58	11.72	31	2.455	1.478	1.410	4.427	1.683	1.520	9.680	0.952	0.959	−0.690
16	5.83	4.32	30	4.092	1.898	1.960	−3.027	3.029	3.084	−1.806	0.935	0.931	0.330
17	7.77	6.17	30	4.092	1.808	1.830	−1.289	2.884	2.542	11.869	0.940	0.947	−0.690
18	9.71	8	30	4.092	1.681	1.710	−1.546	2.625	2.290	12.771	0.949	0.955	−0.619
19	11.64	9.84	30	4.092	1.650	1.580	4.004	2.382	2.155	9.540	0.955	0.961	−0.616
20	13.58	11.67	30	4.092	1.536	1.460	4.856	2.096	2.081	0.727	0.963	0.965	−0.206
21	7.77	6.13	31.5	6.548	1.828	1.870	−2.236	3.724	3.665	1.579	0.952	0.951	0.023
22	9.71	7.96	31.5	6.548	1.750	1.750	−0.101	3.080	3.223	−4.641	0.962	0.960	0.190
23	11.64	9.79	31.5	6.548	1.641	1.640	0.337	2.597	2.880	−10.890	0.970	0.965	0.453
24	13.58	11.62	31.5	6.548	1.575	1.520	3.525	2.406	2.637	−9.600	0.973	0.969	0.390

have strongly criticized their validity in concentration polarization layers of membrane stating that the mechanism of solute transport in these layers is more due to advection than due to convection. Assuming the validity of mass transfer correlations of the standard form, Murthy and Gupta [27] have proposed a graphical method for estimation of k. However, correlations of different form [17,18,28,29] have also been reported in the literature taking the effects of solvent flux, pressure and solute concentration on mass transfer coefficient.

Instead of taking the mass transfer coefficient to be uniform throughout the feed channel length, Sundaramoorthy et al. [1,2] assumed the mass transfer coefficient to vary from inlet to the outlet of the feed channel with varying fluid properties. With this assumption, they proposed a method for estimation of k and applied this method to estimate the mass transfer coefficient using experimental data on the removal of chlorophenol in a laboratory scale spiral wound RO module. They reported that solvent flux and solute concentration have a strong influence on the mass transfer coefficient and proposed a new correlation for mass transfer coefficient accounting for the effects of solvent flux and solute concentration on k.

Experimental readings on the removal of dimethylphenol reported in Tables 2, 3 and 4 are used in this study for the estimation of model parameters A_W, B_S, b and k and the results are reported in this section.

Table 3
Experimental and theoretical data on removal of dimethylphenol in the spiral wound RO module at a feed flow rate of $F_i = 2.330 \times 10^{-4}$ m^3/s.

Sr. no.	P_i (atm)	P_o (atm)	T (°C)	$C_i \times 10^{+03}$ (kmol/m^3)	$F_o \times 10^{+04}$, (m^3/s)		% Error	$C_p \times 10^{+04}$, (kmol/m^3)		% Error	R		% Error
					(Expt)	(Theo)		(Expt)	(Theo)		(Expt)	(Theo)	
1	5.83	4.39	35.5	0.819	1.957	2.060	−5.492	0.915	0.945	−3.301	0.903	0.896	0.684
2	7.77	6.23	35.5	0.819	1.860	1.920	−3.431	0.855	0.845	1.134	0.915	0.913	0.140
3	9.71	8.06	35.5	0.819	1.742	1.780	−2.393	0.742	0.804	−8.347	0.930	0.923	0.793
4	11.64	9.9	35.5	0.819	1.639	1.650	−0.372	0.731	0.788	−7.777	0.935	0.930	0.557
5	13.58	11.73	35.5	0.819	1.542	1.510	2.283	0.622	0.698	−12.219	0.948	0.936	1.319
6	5.83	4.34	31	1.637	2.010	2.080	−3.638	1.519	1.520	−0.048	0.919	0.916	0.282
7	7.77	6.19	31	1.637	1.894	1.950	−2.825	1.289	1.312	−1.748	0.935	0.932	0.298
8	9.71	8.02	31	1.637	1.794	1.810	−1.018	1.193	1.218	−2.083	0.943	0.941	0.178
9	11.64	9.86	31	1.637	1.684	1.680	0.329	1.123	1.172	−4.355	0.949	0.947	0.210
10	13.58	11.68	31	1.637	1.594	1.550	3.071	1.110	1.152	−3.772	0.953	0.952	0.031
11	5.83	4.29	31	2.455	2.022	2.100	−3.778	2.302	2.046	11.131	0.917	0.924	−0.748
12	7.77	6.14	31	2.455	1.907	1.970	−3.135	2.125	1.925	8.988	0.928	0.940	−1.310
13	9.71	7.97	31	2.455	1.815	1.840	−1.122	1.736	1.577	9.162	0.944	0.949	−0.506
14	11.64	9.81	31	2.455	1.707	1.710	0.100	1.640	1.500	8.537	0.950	0.955	−0.470
15	13.58	11.64	31	2.455	1.607	1.580	1.955	1.541	1.460	5.231	0.956	0.959	−0.338
16	5.83	4.25	30	4.092	2.072	2.120	−2.450	2.915	3.057	−4.884	0.936	0.931	0.475
17	7.77	6.1	30	4.092	1.974	2.000	−1.192	2.734	2.490	8.925	0.943	0.947	−0.482
18	9.71	7.92	30	4.092	1.887	1.870	0.794	2.447	2.228	8.947	0.951	0.956	−0.501
19	11.64	9.76	30	4.092	1.805	1.750	3.181	2.227	2.086	6.351	0.957	0.961	−0.415
20	13.58	11.59	30	4.092	1.722	1.620	5.724	1.957	2.004	−2.405	0.964	0.965	−0.120
21	7.77	6.05	31.5	6.548	1.987	2.030	−2.395	3.551	3.599	−1.353	0.953	0.952	0.146
22	9.71	7.88	31.5	6.548	1.902	1.920	−0.745	2.969	3.142	−5.858	0.962	0.960	0.218
23	11.64	9.72	31.5	6.548	1.815	1.800	0.916	2.536	2.800	−10.410	0.969	0.966	0.382
24	13.58	11.54	31.5	6.548	1.734	1.680	3.077	2.342	2.639	−12.680	0.973	0.969	0.340

Table 4
Experimental and theoretical data on removal of dimethylphenol in the spiral wound RO module at a feed flow rate of $F_i = 2.5830 \times 10^{-4}$ m^3/s.

Sr. no.	P_i (atm)	P_o (atm)	T (°C)	$C_i \times 10^{+03}$ (kmol/m^3)	$F_o \times 10^{+04}$, (m^3/s)		% Error	$C_p \times 10^{+03}$, (kmol/m^3)		% Error	R		% Error
					(Expt)	(Theo)		(Expt)	(Theo)		(Expt)	(Theo)	
1	5.83	4.27	35.5	0.819	2.199	2.320	−5.673	0.864	0.926	−7.150	0.907	0.897	1.090
2	7.77	6.11	35.5	0.819	2.075	2.180	−5.218	0.798	0.815	−2.164	0.920	0.915	0.605
3	9.71	7.94	35.5	0.819	1.953	2.040	−4.551	0.626	0.696	−11.180	0.941	0.924	1.773
4	11.64	9.78	35.5	0.819	1.838	1.900	−3.489	0.558	0.608	−8.960	0.950	0.931	2.036
5	13.58	11.61	35.5	0.819	1.720	1.760	−2.487	0.495	0.541	−9.290	0.959	0.936	2.340
6	5.83	4.22	31	1.637	2.261	2.340	−3.591	1.460	1.497	−2.534	0.921	0.916	0.504
7	7.77	6.07	31	1.637	2.148	2.210	−2.694	1.230	1.270	−3.280	0.937	0.933	0.398
8	9.71	7.89	31	1.637	2.041	2.070	−1.372	1.166	1.169	−0.211	0.943	0.942	0.061
9	11.64	9.73	31	1.637	1.947	1.930	0.657	1.116	1.116	0.001	0.948	0.948	−0.035
10	13.58	11.56	31	1.637	1.850	1.800	2.750	1.088	1.089	−0.122	0.951	0.953	−0.184
11	5.83	4.17	31	2.455	2.290	2.360	−2.960	2.279	2.022	11.263	0.917	0.924	−0.812
12	7.77	6.02	31	2.455	2.173	2.220	−2.374	2.000	1.775	11.250	0.931	0.941	−1.089
13	9.71	7.85	31	2.455	2.080	2.090	−0.581	1.670	1.517	9.190	0.944	0.949	−0.519
14	11.64	9.66	31	2.455	1.970	1.960	0.486	1.488	1.432	3.778	0.953	0.955	−0.212
15	13.58	11.51	31	2.455	1.868	1.830	2.111	1.392	1.385	0.539	0.958	0.959	−0.112
16	9.71	7.8	29	4.092	2.113	2.130	−0.666	2.303	2.149	6.698	0.953	0.956	−0.326
17	11.64	9.61	29	4.092	2.070	2.000	3.330	2.120	1.997	5.824	0.958	0.962	−0.389
18	13.58	11.47	29	4.092	1.971	1.870	4.916	1.878	1.906	−1.489	0.965	0.966	−0.121
19	5.83	4.08	31.5	6.548	2.337	2.410	−3.129	3.870	4.298	−11.067	0.946	0.934	1.267
20	7.77	5.93	31.5	6.548	2.253	2.290	−1.685	3.451	3.519	−1.971	0.954	0.952	0.175
21	9.71	7.75	31.5	6.548	2.170	2.170	−0.035	2.896	3.041	−5.014	0.963	0.961	0.206
22	11.64	9.57	31.5	6.548	2.090	2.050	1.853	2.482	2.777	−11.870	0.969	0.966	0.321
23	13.58	11.42	31.5	6.548	2.011	1.930	3.997	2.296	2.614	−13.856	0.973	0.970	0.274

4.1. Estimation of A_w, B_s and b

An equation to calculate the dimensionless parameter ∅ from the measured values F_i, F_o, P_i and P_o was reported by S. Sundaramoorthy et al. [1].

$$\varnothing = \cosh^{-1}\left[\frac{(F_i + F_o) - \beta.F_o}{(F_i + F_o) - \beta F_i}\right] \tag{24}$$

where β is the ratio of pressure drop $(P_i - P_o)$ on the feed channel side to the transmembrane pressure $(P_i - P_P)$ at the feed inlet

$$\beta = \frac{P_i - P_o}{P_i - P_P} \tag{25}$$

The value of ∅ for each one of the experimental readings in Tables 2, 3 and 4 is calculated using Eq. (24).

Eq. (19) indicates that a plot of $(P_i - P_o)$ vs $\frac{L}{\varnothing \sinh \varnothing}[(F_i + F_o)(\cosh\varnothing - 1)]$ is a straight line passing through origin with slope equal to b. The parameter b is estimated by making a straight line fit of data points marked on this plot and evaluating the slope of the line so obtained. For the experimental data reported in this work, the value of b was estimated at $9400.9 \frac{\text{atm.s}}{\text{m}^4}$.

Rewriting the Eq. (13) for ∅ as below

$$\frac{1}{\varnothing^2} = \left(\frac{\gamma}{L^2 W b B_S}\right) T C_p + \left(\frac{1}{L^2 W b A_W}\right) \tag{26}$$

it is evident that a plot of $\frac{1}{\varnothing^2}$ vs $T C_p$ is a straight line with slope S_1 and intercept I_1

$$S_1 = \frac{\gamma}{L^2 W b B_S} \tag{27}$$

$$I_1 = \frac{1}{L^2 W b A_W}. \tag{28}$$

This linear plot shown in Fig. 3 was drawn using the experimental data reported in Tables 2, 3 and 4. The slope S_1 and intercept I_1 of the best linear fit were evaluated by the method of least squares and values of model parameters A_w and B_s were estimated using Eqs. (27) and (28). The estimated values of model parameters are $A_w = 9.7388 \times 10^{-7}$ and $B_s = 1.5876 \times 10^{-8}$. The experimental data points were observed to fit the straight line with regression coefficient R^2 equal to 0.89. The values of estimated model parameters are given in Table 5.

4.2. Estimation of mass transfer coefficient k

The value of mass transfer coefficient k is assumed to vary from one end to the other end of the feed channel with varying conditions of pressure, flow rate, and solute concentration. So, for each one of the experimental readings reported in Tables 2, 3 and 4, two values of mass transfer coefficients, one at feed inlet and the other at feed outlet, are calculated using the equations given below at feed inlet (x = 0),

$$k = \frac{J_V(0)}{ln\left[\frac{J_V(0)}{B_S}\left(\frac{C_p}{C_i - C_p}\right)\right]} \tag{29}$$

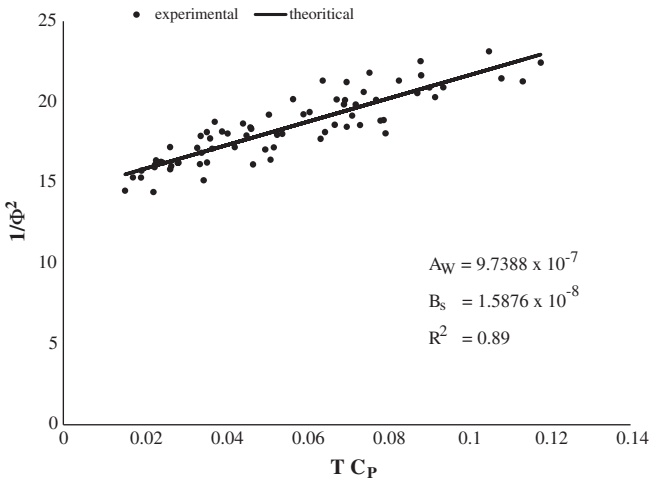

Fig. 3. Plot of $\frac{1}{\varnothing^2}$ vs $T C_p$ for estimation of A_w and B_s.

Table 5
Value of model parameters A_W, B_S and b.

Parameter	Value
$b\ \frac{atm.s}{m^4}$	9400.9
$A_W\ \frac{m}{atm.s}$	9.7388×10^{-7}
$B_S\ \frac{m}{s}$	1.5876×10^{-8}

at feed outlet (x = L),

$$k = \frac{J_V(L)}{ln\left[\frac{J_V(L)}{B_S}\left(\frac{C_p}{C_o - C_p}\right)\right]}. \quad (30)$$

The equations listed above are derived by rearranging the terms in Eqs. (21) and (22). The values of solvent flux $J_v(0)$ and $J_v(L)$ appearing in the above equations are calculated using Eqs. (14) and (15). A total of 142 values of k were calculated using 71 experimental readings reported in Tables 2, 3 and 4.

Accounting for the influences of solvent flux J_v, solute concentration C_b and fluid velocity v_f on mass transfer coefficient k, Sundaramoorthy et al. [2] have proposed a correlation for mass transfer coefficient written in the form

$$Sh = a\, Re_p^{n1} c_m^{n2} Re_f^{n3} \quad (31)$$

where dimensionless numbers appearing in this correlation are defined as follows

$$sh = \textit{Sherwood Number} = \frac{kd_e}{D_A} \quad (32)$$

$$Re_p = \textit{Permeate Reynolds Number} = \frac{\rho d_e J_v}{\mu} \quad (33)$$

$$C_m = \textit{Dimensionless solute concentration} = \frac{C_b}{\rho_m} \quad (34)$$

$$Re_f = \textit{Fluid Reynolds Number} = \frac{\rho\, d_e\, v_f}{\mu} \quad (35)$$

Here d_e is the equivalent diameter of the rectangular feed channel of thickness t_f

$$d_e = 2\, t_f \quad (36)$$

and ρ_m is the molal density of water (55.56 kmol/m^3). The Permeate Reynolds number Re_p in Eq. (33) is defined to account for the influence of solvent flux J_v on k.

The coefficient 'a' and the exponents n1, n2 and n3 in Eq. (31) were estimated using 142 values of k calculated from the 71 experimental readings reported in Tables 2, 3 and 4 by the method of least squares. The final correlation for mass transfer coefficient

$$Sh = 246.9\, Re_p^{0.803} c_m^{0.129} Re_f^{0.101} \quad (37)$$

obtained from the experimental data on the removal of dimethylphenol is shown to fit the data (Fig. 4) with a regression coefficient R^2 value equal to 0.99. Comparing this correlation with the one reported by Sundaramoorthy et al. [2] for the experimental data on the removal of chlorophenol,

$$Sh = 147.4\, Re_p^{0.739} c_m^{0.135} Re_f^{0.130} \quad (38)$$

it is observed that the respective values of the exponents of Re_p, c_m and Re_f in both the correlations (Eqs. (37) and (38)) are very close to one another and they differ only by a very small margin of around 10%. These results justify the validity of the correlation (Eq. (31)) for both the phenolic compounds namely chlorophenol and dimethylphenol. The Eqs. (37) and (38) obtained for these two phenolic compounds can be combined to give a single correlation of the form

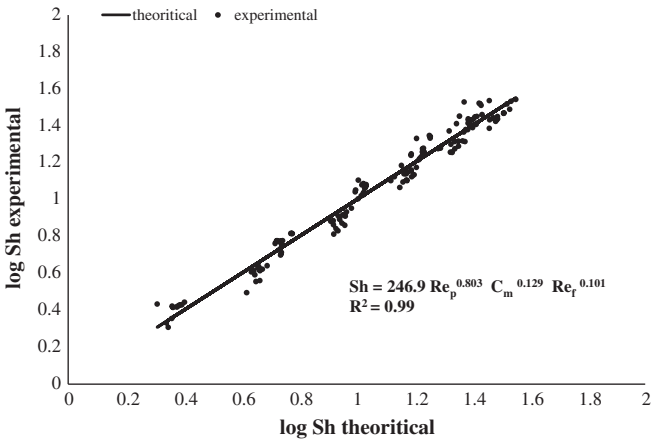

Fig. 4. Linear fit of experimental data with mass transfer correlation.

$$Sh = a^1\, Sc^{n0} Re_p^{n1} c_m^{n2} Re_f^{n3} \quad (39)$$

where the Schmidt Number Sc $\left(Sc = \frac{\mu}{\rho D_A}\right)$ term in the correlation is introduced to account for the effect of solute properties on mass transfer coefficient k. The values of the parameters a^1 and n0 in Eq. (39) can be estimated by the method of least squares using the experimental readings reported in this study for dimethylphenol along with the experimental data reported by Sundaramoorthy et al. [2] for chlorophenol. However, in order to get a reliable estimate of these two parameters a^1 and n0, experiments similar to the one reported in this study are to be performed with more number of organic solutes. Experiments are required to be carried out with at least one more organic solute in order to propose a correlation of the form given by Eq. (39).

5. Validation of the model with experimental data

Once validated with experimental data, the mathematical model can be used as a tool to analyze the performance of a spiral wound RO module under various operating conditions. The model can predict the values of retentate pressure P_o, retentate flow F_o, retentate concentration C_o, permeate concentration C_p and rejection coefficient R for a given set of values of feed pressure P_i, feed flow rate F_i,feed concentration C_i, permeate pressure P_p and feed temperature T.

The iterative calculation steps (algorithm) for model predictions are outlined here.

- Step 1: Assume permeate concentration $C_p = C_{pa}$ (Initial guess for $C_{pa} = 0.5 * C_i$)
- Step 2: Calculate ∅ using Eq. (13)
- Step 3: Calculate ΔP_i using Eq. (16)
- Step 4: Calculate F_o using Eq. (18)
- Step 5: Calculate P_o using Eq. (19)
- Step 6: Calculate ΔP_o using Eq. (17)
- Step 7 Calculate $J_v(0)$ and $J_v(L)$ using Eqs. (14) and (15)
- Step 8: Calculate the fluid velocities $v_{fi} = F_i/A_f$ and $v_{fo} = F_o/A_f$ (A_f is feed channel area)
- Step 9: Calculate C_o using Eq. (20)
- Step 10: Calculate Re_p, C_m and Re_f using Eqs. (33), (34) and (35) at inlet and outlet

- Step 11: Calculate k at inlet (k_i) and outlet (k_o) using the correlation (37)
- Step 12: Calculate C_p at inlet (C_{pi}) and at outlet (C_{po}) using Eqs. (21) and (22)
- Step 13: Calculate $C_p = 0.5 * (C_{pi} + C_{po})$
- Step 14: Compare calculated C_p (step 13) with assumed C_p ($= C_{pa}$) On convergence of calculated C_p to assumed C_p, go to Step 16 else go to Step 15
- Step 15: Assume new value of C_{pa} as $C_{pa} = 0.5(C_p + C_{pa})$ and Go to Step 1
- Step 16: Calculate $F_p = F_i - F_o$
- Step 17: Calculate R using Eq. (23)

A computer program was developed in MATLAB language to execute this algorithm. Using this calculation procedure, the values of retentate flow F_o, retentate pressure P_o, retentate concentration C_o, permeate concentration C_p and rejection coefficient R estimated by the model were calculated for each one of the readings in Tables 2, 3 and 4. The model parameter values listed in Table 5 for A_w, B_s and b were used in these calculations. The mass transfer correlation (Eq. (37)) applicable for dimethylphenol was used for estimation of k.

The predicted values of F_o, C_p and R are listed in Tables 2, 3 and 4 along with the experimental readings. Comparison of the predicted values of F_o, C_p and R with the corresponding experimental readings show that the model is able to predict the values of retentate flow F_o within 5% error for 90% of the readings, permeate concentration C_p within 12% error for 93% of the readings and rejection coefficient R within 2% error for 97% of the readings. Theoretical model predictions of retentate concentration C_o and retentate pressure P_o are in good agreement with the experimental readings as shown in Figs. 5 and 6. Thus the experimental data reported in this work on the removal of dimethylphenol in a spiral wound RO module validates the analytical model developed by Sundaramoorthy et al. [1] within reasonable error.

6. Conclusions

An analytical model for spiral wound RO modules was developed and reported recently by Sundaramoorthy et al. [1] assuming spatial variations of pressure, flow and solute concentration in the feed channel and uniform pressure in the permeate channel. They further conducted some experimental studies [2] on the removal of chlorophenol in a laboratory scale spiral wound RO module and validated the analytical model with the experimental data. In this research paper, experimental studies conducted on the same spiral wound RO module taking a feed solution containing a different organic solute namely dimethylphenol is reported. The main objective of this research work was to verify if the analytical model reported by Sundaramoorthy et al. [1] also holds for feed solutions containing another phenolic compound namely dimethylphenol.

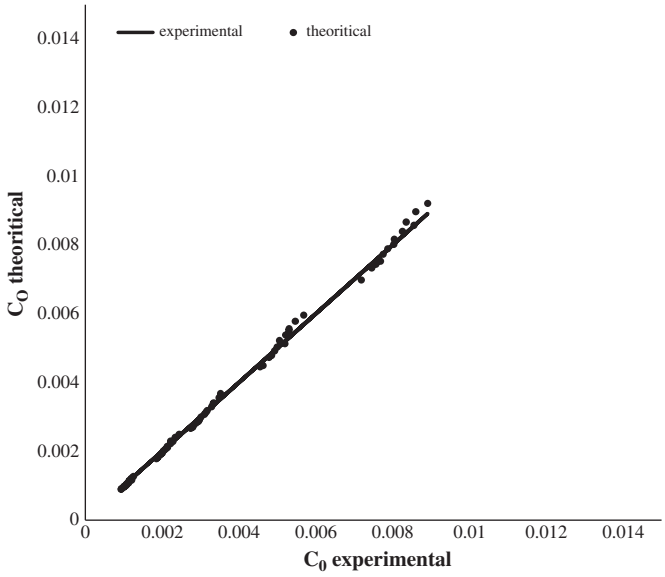

Fig. 5. Comparison of theoretical and experimental values of C_o.

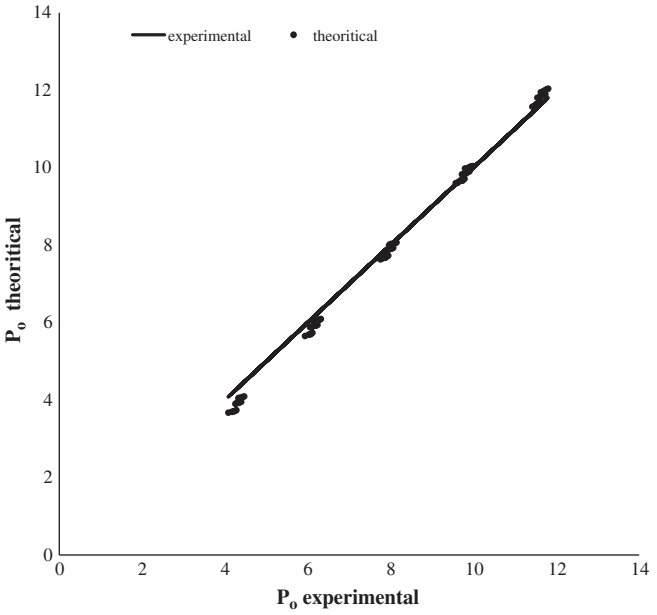

Fig. 6. Comparison of theoretical and experimental values of P_o.

A total of 71 experimental readings were collected and reported in this work by conducting experiments in which feed flow rate, feed concentration and feed pressure were varied and the readings of retentate flow rate, retentate concentration, retentate pressure and permeate concentration were recorded. Using these experimental readings, four model parameters namely solvent transport coefficient A_w, solute transport coefficient B_s, feed channel friction coefficient b and the mass transfer coefficient k were estimated.

A comparison of the values of model parameters estimated in this work for dimethylphenol data with the values reported by Sundaramoorthy et al. [2] for chlorophenol data reveals the following:

i) The value of solvent transport coefficient A_w estimated for the dimethylphenol data ($A_w = 9.7388 \times 10^{-7}$) is very close to the value estimated for the chlorophenol data ($A_w = 9.5188 \times 10^{-7}$) asserting the fact that the solvent transport coefficient A_w is independent of solute properties and depends only on the nature of the solvents and the characteristics of the membrane used.

ii) The value of solute transport coefficient B_s estimated for dimethylphenol ($B_s = 1.5876 \times 10^{-8}$) is about five times lower than the value reported for chlorophenol ($B_s = 8.468 \times 10^{-8}$). It means that chlorophenol can permeate faster through the polyamide membrane than dimethylphenol. This is reflected in the higher values of rejection coefficient R ranging between 90% and 97% reported for dimethylphenol (Tables 2, 3 and 4) compared to values of R ranging from 58% to 82% for chlorophenol [2].

iii) The value of feed channel friction coefficient b estimated for the dimethylphenol data ($b = 9400.9$) is about 10% higher than the value estimated for the chlorophenol data ($b = 8529.5$). Although the value of b is influenced by the viscosity of the fluids, this effect can be neglected for dilute aqueous solutions

and so b is taken to be dependent only on module dimensions and geometry.

iv) Similar to what is reported by Sundaramoorthy et al. [2] for the chlorophenol data, the values of mass transfer coefficient k estimated in this study for the dimethylphenol data are found to be influenced not only by the fluid velocity v_f but also by solvent flux J_v and solute concentration C. Taking the influences of fluid velocity v_f, solvent flux J_v and solute concentration C on the mass transfer coefficient k, a correlation of the form

$$Sh = a\, Re_p^{n1} c_m^{n2} Re_f^{n3} \quad (40)$$

was reported to fit the experimental data well with regression coefficient R^2 value of the fit equal to 0.99. Further, the estimated values of the exponents n1, n2 and n3 in the correlation obtained for the 'chlorophenol data' are nearly equal to the corresponding values of the exponents in the correlation obtained for the 'dimethylphenol data' (Eqs. (37) and (38)).

A test on the predictive capability of the analytical model in validating the experimental data on the removal of dimethylphenol proved that the model was capable of predicting the performance of spiral wound RO module within 5% error for retentate flow F_o, 12% error for permeate concentration C_p and 2% error for rejection coefficient R. These results are similar to the one reported by Sundaramoorthy et al. [2] for the chlorophenol data.

The results presented in this study clearly prove the consistency of the analytical model in predicting the performances of spiral wound RO modules with both the feed solutions containing dimethylphenol and the feed solutions containing chlorophenol. It is also suggested in this work that a modified form of the proposed correlation for mass transfer coefficient k, incorporating Schmidt Number Sc to account for the solute properties, can be obtained by conducting at least one more set of experiments, similar to the one reported in this study, taking feed solutions containing a different organic solute. Such experiments with feed solution containing 'phenol' as a solute are in progress and will be reported in future by the authors of this research paper.

Symbols

a	coefficient appearing in Eq. (31)
a^1	coefficient appearing in Eq. (39)
A_f	feed channel area (m^2)
A_m	membrane area (m^2)
A_p	permeate channel area (m^2)
A_w	solvent transport coefficient (m/atm.s)
b	feed channel friction parameter (atm.s/m^4)
B_s	solute transport coefficient (m/s)
C	solute concentration in feed channel (kmol/m^3)
C_b	bulk solute concentration in the feed channel (kmol/m^3)
C_i	concentration of solute in the feed (kmol/m^3)
C_o	concentration of solute in the retentate (kmol/m^3)
C_p	concentration of solute in the permeate (kmol/m^3)
C_{pa}	assumed value of C_p in the iterative calculation steps (kmol/m^3)
C_{pi}	value of C_p at module inlet (kmol/m^3)
C_{po}	value of C_p at module outlet (kmol/m^3)
C_m	dimensionless solute concentration in Eq. (34)
C_w	concentration of solute at the membrane wall (kmol/m^3)
d_e	equivalent diameter of feed channel (m)
D	module diameter (m)
D_A	diffusivity (m^2/s)
F_i	feed flow rate (m^3/s)
F_p	permeate flow rate (m^3/s)
F_o	retentate flow rate (m^3/s)
I_1	intercept of the straight line plot corresponding to Eq. (26)
J_S	solute flux (kmol of solute/m^2s)
J_V	solvent flux (m/s)
K	mass transfer coefficient (m/s)
k_i	mass transfer coefficient at the inlet (m/s)
k_o	mass transfer coefficient at the outlet (m/s)
L	RO module length (m)
n	number of turns in the spiral wound module
P_b	pressure in the feed channel (atm)
P_i	pressure at the feed inlet (atm)
P_o	pressure at the feed channel outlet (atm)
P_p	pressure in the permeate channel (atm)
n0	exponent of Schmidt number appearing in Eq. (39)
n1	exponent of permeate Reynolds number appearing in Eqs. (31) and (39)
n2	exponent of dimensionless solute concentration appearing in Eqs. (31) and (39)
n3	exponent of fluid Reynolds number appearing in Eqs. (31) and (39)
R	rejection coefficient
Re_p	permeate Reynolds number in Eq. (33)
Re_f	fluid Reynolds number in Eq. (35)
Sh	Sherwood Number in Eq. (32)
Sc	Schmidt Number in Eq. (39)
S_1	slope of the straight line plot corresponding to Eq. (26)
t_f	feed spacer thickness, mm
t_P	permeate channel thickness, mm
T	temperature (K)
v_f	fluid velocity in feed channel (m/s)
v_{fi}	fluid velocity at channel inlet (m/s)
v_{fo}	fluid velocity at channel outlet (m/s)
W	RO module width (m)
x	axial position in feed channel

Greek symbols

β	a dimensionless parameter, defined in Eq. (25)
Δ	difference across the membrane
ϕ	dimensionless term defined in Eq. (13)
γ	gas law constant $\left(\gamma = R, 0.0820 \ \frac{atm\ m^3}{°K\ kmol}\right)$
μ	viscosity (kg/ms)
Π	osmotic pressure (atm)
ρ	fluid density (kg/m^3)
ρ_m	molal density of water (55.56 kmol/m^3)

References

[1] S. Sundaramoorthy, G. Srinivasan, D.V.R. Murthy, An analytical model for spiral wound reverse osmosis membrane modules: part-1-Model development and Parameter estimation, Desalination (2011), doi:10.1016/j.desal.2011.03.047.

[2] S. Sundaramoorthy, G. Srinivasan, D.V.R. Murthy, An analytical model for spiral wound reverse osmosis membrane modules: part-II — experimental validation, Desalination 277 (2011) 257–264.

[3] A. Bodalo-Santoyo, J.L. Gomez-Carasco, E. Gomez-Gomez, M.F. Maximo-Martin, A.M. Hidalgo-Montesinos, Application of reverse osmosis membrane to reduce pollutants present in industrial waste water, Desalination 155 (2003) 101–108.

[4] Y. Yoon, R.M. Lupetow, Removal of organic contaminants by RO and NF membranes, J. Membr. Sci. 261 (2005) 76–86.

[5] S. Sourirajan, T. Matsuura, Physicochemical criteria for reverse osmosis separation of alcohols, phenols and monocarboxylic acids in aqueous solutions using porous cellulose acetate membranes, J. Appl. Polym. Sci. 15 (1971) 2905–2927.

[6] S. Sourirajan, T. Matsuura, P. Blais, J.M. Dickson, Reverse osmosis separations for some alcohols and phenols in aqueous solutions using aromatic polyamide membranes, J. Appl. Polym. Sci. 18 (1974) 3671–3684.

[7] T. Matsuura, Y. Fang, S. Sourirajan, Reverse osmosis separation of binary organic mixtures using cellulose acetate butyrate and aromatic polyamide membranes, J. Appl. Polym. Sci. 44 (1992) 1959–1969.

[8] F.C. Schutte, The rejection of specific organic compounds by reverse osmosis membranes, Desalination 158 (2003) 285–294.

[9] A. Bodalo-Santoyo, J.L. Gomez-Carasco, E. Gomez-Gomez, M.F. Maximo-Martin, A.M. Hidalgo-Montesinos, Spiral-wound membrane reverse osmosis and the treatment of industrial effluents, Desalination 160 (2004) 151–158.
[10] D. Bhattacharyya, M. Williams, Introduction and definitions — reverse osmosis, in: W. Ho, K. Sirkar (Eds.), Membrane Handbook, Van Nostrand Reinhold, New York, 1992, pp. 265–268.
[11] D. Bhattacharyya, M. Williams, Theory — reverse osmosis, in: W. Ho, K. Sirkar (Eds.), Membrane Handbook, Van Nostrand Reinhold, New York, 1992, pp. 269–280.
[12] A. Allegrezza, Commercial reverse osmosis membranes and modules, in: B. Parekh (Ed.), Reverse Osmosis Technology, Marcel Dekker, Inc., New York, 1988, pp. 53–120.
[13] K.K. Sirkar, P.T. Dong, G.H. Rao, Approximate design equations for reverse osmosis desalination by spiral wound modules, Chem. Eng. Sci. 21 (1982) 517–527.
[14] S.K. Gupta, Analytical design equations for reverse osmosis systems, Ind. Eng. Chem. Process. Des. Dev. 24 (1985) 1240.
[15] F. Evangelista, G. Jonsson, Optimum design and performance of spiral wound modules II: analytical method, Chem. Eng. Commun. 72 (1988) 83–94.
[16] F. Evangelista, A short cut method for the design of reverse osmosis desalination plants, Ind. Eng. Chem. Process. Des. Dev. 24 (1985) 211–223.
[17] S. Avlonitis, W.T. Hanbury, M. Ben Boudinar, Spiral wound modules performance. An analytical solution: part I, Desalination 81 (1991) 191–208.
[18] S. Avlonitis, W.T. Hanbury, M. Ben Boudinar, Spiral wound modules performance. An analytical solution: part II, Desalination 89 (1993) 227–246.
[19] H. Lonsdale, E.A. Mason, Statistical–mechanical theory of membrane transport, J. Membr. Sci. 51 (1990) 1–81.
[20] V. Gekas, B. Hallstrom, Mass transfer in the membrane concentration polarization layer under turbulent cross flow. I, Critical literature review and prediction of existing Sherwood correlations to membrane operations, J. Membr. Sci. 30 (1987) 153.
[21] P.C. Wankat, Rate-Controlled Separations, Springer International, 1994.
[22] G. Schock, A. Miquel, Mass transfer and pressure loss in spiral wound modules, Desalination 64 (1987) 339–352.
[23] Z.V.P. Murthy, S.K. Gupta, Estimation of mass transfer coefficient using a combined nonlinear membrane transport and film theory model, Desalination 109 (1997) 39–49.
[24] A. Chiolle, G. Gianotti, M. Gramondo, G. Parrini, Mathematical model of reverse osmosis in parallel-wall channels with turbulence promoting nets, Desalination 26 (1978) 3.
[25] G. Belfort, N. Negata, Fluid mechanics and cross-filtration filtration: some thoughts, Desalination 53 (1985) 57.
[26] G. Jonsson, Boundary layer phenomenon during ultrafiltration of dextran and whey protein solutions, Desalination 51 (1984) 61.
[27] Z.V.P. Murthy, S.K. Gupta, Simple graphical method to estimate membrane transport parameters and mass transfer coefficient in a membrane cell, Sep. Sci. Technol. 31 (1996) 77–94.
[28] P. Erikson, Water and Salt transport through two types of polyamide composite membranes, J. Membr. Sci. 36 (1988) 297–313.
[29] V. Geraldes, V. Semilao, M.N. Pinho, Flow and mass transfer modelling of nanofiltration, J. Membr. Sci. 191 (2001) 109–128.